Multi-Physics Simulations for the Design of Probe-Heads Micro-Needles

A. Corigliano[*1], A. Courard[1], G. Cocchetti[1], L. Magagnin[2], R. Vallauri[3] and D. Acconcia[3]

[1]Department of Structural Engineering, Politecnico di Milano
[2]Department of Chemistry, Materials and Chemical Engineering, Politecnico di Milano
        Piazza Leonardo da Vinci, 32 - 20133 Milano, Italy.
[3]Technoprobe SPA
        Via Cavalieri di Vittorio Veneto, 2 - 23870 Cernusco Lombardone, Italy.
*Corresponding author: Piazza Leonardo da Vinci, 32 - 20133 Milano, Italy, alberto.corigliano@polimi.it

Abstract: The paper presents recent results concerning the experimental mechanical characterization, the numerical modeling and the design of micro-needles used in the construction of probe heads for wafer testing. A fully coupled electro-thermal model was created using COMSOL and combined to a research-oriented thermo-mechanical Finite Element (FE) code in order to accurately reproduce the micro-needle behavior under constant load and varying current intensity. The numerical simulations put in evidence the influence of the presence of a set of micro-needles on the temperature distribution.

Keywords: Joule heating interface, electro-thermo-mechanical simulations, wafer testing.

1. Introduction

During wafer testing of electronic and other microsystem devices, contact between probe-head and pads, and the closing of the electric circuit are assured by micro-needles that can be considered as beams in a buckled regime (Figure. 1).
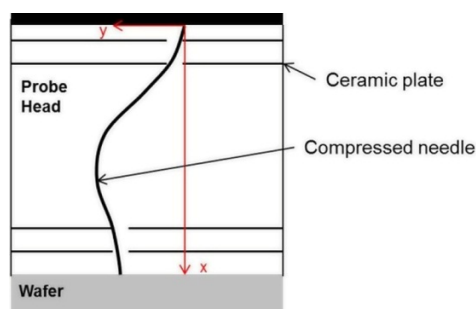

Figure 1. Probe-head micro-needle

The micro-needles must show high mechanical and electrical performances: high flexibility, high electrical conductivity and high resistance to electro-thermo-mechanical fatigue.

The correct design of micro-needles can be obtained only making use of accurate multi-physics simulations in which thermal, electrical and mechanical responses are correctly simulated in a fully coupled environment.

2. Use of COMSOL Multiphysics

A fully coupled electro-thermal finite elements model of the micro-needles was defined using the Joule heating interface. Due to the fact that the micro-needles can be subject to high currents (over 1 A for a cross-section in the order of 40x40 μm^2) and consequently high temperatures, the variation of the electrical resistivity ρ with the temperature T must be considered in the model. The electrical resistivity was assumed to be a linear function of the temperature:

$$\rho(T) = \rho_0\left[1 + \alpha_{res}\left(T - T_{ref}\right)\right] \qquad (1)$$

where

* T_{ref}: reference temperature (K)

* ρ_0:   electrical resistivity at T_{ref} (Ω m)

* α_{res}: temperature coefficient of resistivity (1/K)

The two main causes of heat dissipation are the anchors and the surrounding air. The four intermediate ceramic plates (see Figure 1) were not taken into account in the model. Indeed, their thermal diffusivities are so small with respect to the thermal diffusivities of the bottom and upper plates, that the dissipation due to the contacts between the micro-needle and the intermediate plates can be neglected.

The model makes use of a stationary analysis and gives as output the temperature distribution along the needle. The simulation was repeated for various configurations: a single needle, a

regular grid of nine needles and a regular grid of 100 needles. As a consequence, it was possible to understand how the presence of other micro-needles influences the temperature distribution. In the cases where a grid of needles was studied, the Rayleigh number was computed, which allows to compare the free convection with the conduction regimes. For a Rayleigh number less than 2000, the convection can be neglected with respect to the conduction.

Rayleigh number

$$Ra = Gr * Pr = \frac{g\beta}{\nu\alpha_{th}}(T_s - T_\infty)\delta^3 \qquad (2)$$

where

* Gr: Grashof number
* Pr: Prandtl number
* g: acceleration due to gravity (m.s^{-2})
* β: thermal expansion coefficient (K^{-1})
* ν: kinematic viscosity (m^2.s^{-1})
* α_{th}: thermal diffusivity (m^2.s^{-1})
* T_s: temperature on the surface of the needle (K)
* T_∞: fluid temperature far from the surface of the needle (K)
* δ: needle length (m)

Inside the grid, the Rayleigh number is less than 0.02 due to the small distances between needles, the convection in the air can be therefore neglected. Hence the convection was taken into account for the external needles only.

It was supposed that far from the micro-needle the temperature of the upper and bottom plates were constant. So the temperature of the lateral faces of the upper and bottom plates was fixed at 20°C.

Simulations evidenced higher temperature values in the presence of several needles with respect to the case with a single needle (Figures 2, 3). The hot needles reduce the surrounding air cooling thus decreasing the heat dissipation by conduction in the air. Consequently, the maximum current that a micro-needle can sustain will be reduced.
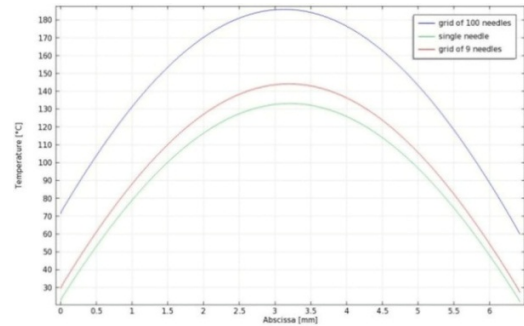

Figure 2. Temperature along the central micro-needle for a 1 A current

In a second step, the results in terms of temperature distribution obtained with the coupled multi-physics simulation were used as input for a research-oriented thermo-mechanical FE code for the needles treated as slender beams. The influence of the temperature on the mechanical properties (Young's modulus, yield stress) was taken into account. The Young's modulus and the yield stress were supposed to follow a linear function of the temperature. Furthermore, as the deflection of the needle is large, the Von Kármán hypothesis on the strain was used:

$$\varepsilon_x = \frac{du}{dx} + \frac{1}{2}\left(\frac{dw}{dx}\right)^2 - y\frac{d^2w}{dx^2} \qquad (3)$$

where

* ε_x: strain
* u: horizontal displacement (m)
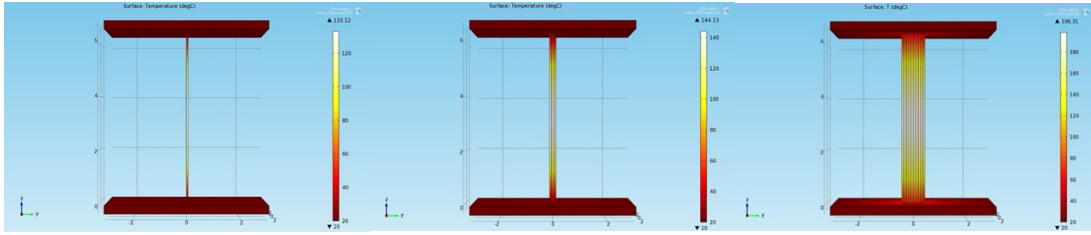* w: vertical displacement (m)

Figure 3. Results of the electro-thermal simulations

With these assumptions, the thermo-mechanical behavior of the micro-needle is governed by the following system:

$$
\begin{cases}
E(T)A\left(\dfrac{du}{dx}+\dfrac{1}{2}\left(\dfrac{dw}{dx}\right)^2-\alpha\Delta T\right)+P=0 \\[2ex]
\dfrac{d^2}{dx^2}\left(E(T)J\dfrac{d^2w}{dx^2}\right)- \\[2ex]
-\dfrac{d}{dx}\left[E(T)A\dfrac{dw}{dx}\left(\dfrac{du}{dx}+\dfrac{1}{2}\left(\dfrac{dw}{dx}\right)^2-\alpha\Delta T\right)\right]=0
\end{cases}
\qquad (4)
$$

where:

∗ $E(T)$: Young's modulus (Pa)
∗ A: cross-section area (m^2)
∗ ΔT. temperature gradient (K)
∗ J: moment of inertia (m^4)
∗ P: force applied at the micro-needle extremity (N)

It has to be noticed that, as the temperature varies along the micro-needle (the extremities are colder than the center), so do the Young's modulus and the yield stress. We used Euler-Bernoulli elements to solve the system above.

Moreover the elastic-plastic behavior of the material was modeled introducing plastic hinges, which are activated when the stress becomes higher than the yield stress.

The contacts between the micro-needle and the intermediate ceramic plates were implemented as simple supports.
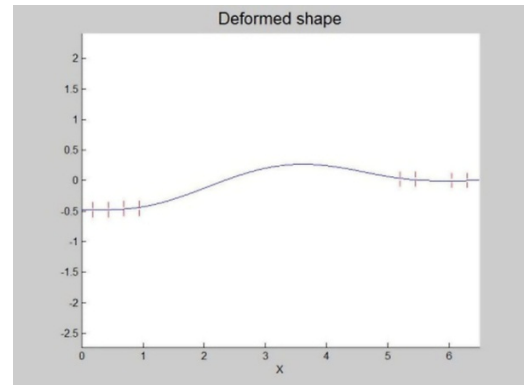

Figure 4. Results of the thermo-mechanical simulation (in mm)

The two FE models combined were used to numerically reproduce the so-called CCC (Current Carrying Capability) test, which consists in the measurement of the reaction force of a single compressed needle subject to an increasing direct current. The CCC test is the standard used by industry to characterize needles performance. The CCC is then defined as the current associated to a decreasing of 20% of the reaction force. For higher currents, the micro-needle is irreversibly deformed.

The CCC test was modeled with success (Figure 5.). As the current increases, the force decreases due to the reduction of the Young's modulus with temperature. At the end of the test, the micro-needle is plastically deformed; this fact is explained by the reduction of the yield stress with temperature. It can be noticed that, as electro-thermal simulations on micro-needles grid showed previously, the CCC will be reduced. Plasticization will occur for a lower current when the micro-needle is inside a grid of other micro-needles due to higher temperature.
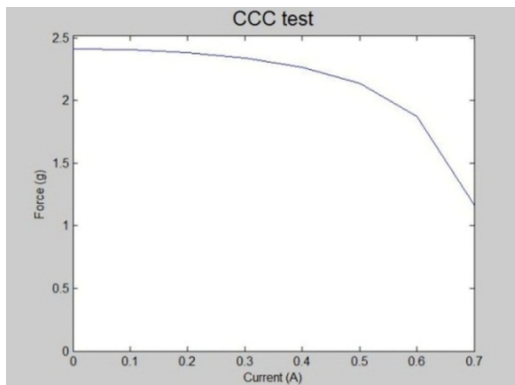
Figure 5. CCC test of a micro-needle

7. Conclusions

The combined use of multi-physics simulations obtained with COMSOL Multi-Physics and of a research oriented FE code allowed to numerically simulate the CCC test. It was possible to show that the CCC can be reduced by an important amount in the case of a grid of micro-needles with respect to the single needle configuration. The tools formulated for the numerical simulation in coupled electro-thermo-mechanical conditions can be of great help in the design of probe-heads micro needles.

8. References

1. Augier, D., More**, C.**, *Physique 2ème année MP MP* PT PT**, pp. 771-817, TEC&DOC, Paris (2004)
2. Corradi dell'Acqua, L., *Meccanica delle strutture: la valutazione della capacità portante*, pp. 205-245, McGraw-Hill, Milan (1994)
3. Reddy, J. N., *An introduction to the finite element method*, pp. 594-596, McGraw-Hill, Austin (1993)
4. Kirby. R, Yan H. F., New Methodology for Probe CCC Cahracterization, *South West Test Workshop* (2004)
5. Zeman M., A New Methodology for Assessing the Current Carrying Capability of Probes Used at Sort, *IEEE SW Test Workshop* (2010)
6. Kister J., Hopkins S., MicroProbe Vx-MP Probe Card Technology, *IEEE SW Test Workshop* (2008)
7. Slessor M., Marshall M., A Flexible Verticak MEMs Probe Card Technology for Pre-Bump and eWLP Applications, *IEEE SW Test Workshop* (2011)
8. Wittig A., Leong A, Hulic D., Evaluation of New Probe Technology on SnAg and Copper Bumps, *IEEE SW Test Workshop* (2011)
9. Kister J., Key design Parameters to Maximize Probe Current Carrying Capability, *IEEE SW Test Workshop* (2011)
10. Nagler O., Degen C., Nouri M., Kister J., Slessor M., MicroProbe Vx-Rf Probe Card Technology, *IEEE SW Test Workshop* (2009)
11. Gonzales D. E, Kister J., Advancements in Performance of Buckling Beam Probes, *South West Test Workshop* (1999)
12. Liu Y., Desbiens D., Luk T., Irving S., Parameter Optimization for Wafer Probe Using Simulation, *EuroSimE* (2005)